



Optimization and synthesis of multilayer frequency selective surfaces via bioinspired hybrid techniques

Wirlan Gomes Lima; Jasmine Priscyla Leite de Araújo; Fabrício José Brito

Barros; Gervásio Protásio dos Santos Cavalcante; Cássio da Cruz Nogueira; Bruno Souza

Lyra Castro; Miércio Cardoso de Alcântara Neto

Abstract

In this study, two bioinspired computation (BIC) techniques are discussed and applied to the project and synthesis of multilayer frequency selective surfaces (FSS) within the microwave band, specifically for C, X and Ku bands. The proposed BIC techniques consist of combining a general regression neural network to a genetic algorithm and a cuckoo search algorithm, respectively. The objective is to find the optimal values of separation between the investigated FSS. Numerical analysis of the electromagnetic properties of the device is made possible with the finite integration method and validated through the finite element method, utilizing both softwares CST Microwave Studio and Ansys HFSS respectively. Thus, the BIC-optimized devices presents good phase / angular stability for angles 10°, 20°, 30° and 40°, as well as being polarization independent. The cutoff frequencies to control the operating frequency range of the FSS, referring to transmission coefficient in decibels (dB), were obtained at a threshold of -10dB. Numerical results denote good accordance with measured data.

Keyword: hybrid optimization methods; FSS; GRNN; MOGA; MOCS.

Published Date: 5/1/2020

Page.542-561

Vol 8 No 05 2020

DOI: <https://doi.org/10.31686/ijer.vol8.iss5.2371>

Optimization and synthesis of multilayer frequency selective surfaces via bioinspired hybrid techniques

Wirlan Gomes Lima (Corresponding author)

Telecommunication and Computation Laboratory, Federal University of Pará,
Belém, Pará, Brazil.
e-mail: wirlan.lima-17@hotmail.com

Jasmine Priscyla Leite de Araújo

Telecommunication and Computation Laboratory, Federal University of Pará
Belém, Pará, Brazil.

Fabício José Brito Barros

Telecommunication and Computation Laboratory, Federal University of Pará
Belém, Pará, Brazil.

Gervásio Protásio dos Santos Cavalcante

Telecommunication and Computation Laboratory, Federal University of Pará
Belém, Pará, Brazil.

Cássio da Cruz Nogueira

Telecommunication and Computation Laboratory, Federal University of Pará
Belém, Pará, Brazil.

Bruno Souza Lyra Castro

Telecommunication and Computation Laboratory, Federal University of Pará
Belém, Pará, Brazil.

Miércio Cardoso de Alcântara Neto

Telecommunication and Computation Laboratory, Federal University of Pará
Belém, Pará, Brazil.

Abstract

In this study, two bioinspired computation (BIC) techniques are discussed and applied to the project and synthesis of multilayer frequency selective surfaces (FSS) within the microwave band, specifically for C, X and Ku bands. The proposed BIC techniques consist of combining an general regression neural network to a genetic algorithm and a cuckoo search algorithm, respectively. The objective is to find the optimal values of separation between the investigated FSS. Numerical analysis of the electromagnetic properties of the

device is made possible with the finite integration method and validated through the finite element method, utilizing both softwares CST Microwave Studio and Ansys HFSS respectively. Thus, the BIC-optimized devices presents good phase / angular stability for angles 10° , 20° , 30° and 40° , as well as being polarization independent. The cutoff frequencies to control the operating frequency range of the FSS, referring to transmission coefficient in decibels (dB), were obtained at a threshold of -10dB . Numerical results denote good accordance with measured data.

Keywords: hybrid optimization methods; FSS; GRNN; MOGA; MOCS.

1. Introduction

Bioinspired computation (BIC) consists of a new computer science paradigm inspired by certain behaviors of living beings. These ideas, extracted from natural systems, is already being successfully utilized for the development of technological tools capable of solving high-complexity general problems in engineering and industry [1–2].

This theme possesses a multidisciplinary character and an abundance of applications. The growing interest of researchers within the electromagnetism community is due to BIC's adaptability, as well as its self-organization tendencies and tolerance to random defects [2–4]. Examples of widely applied, successful algorithms are the classic genetic algorithm (GA), artificial neural networks (ANN) and particle swarm optimization (PSO) [5].

With the intent of combining the main advantages of these classic algorithms researchers are proposing new meta-heuristic techniques, aiming to both accelerate project development or enhance the characteristics of projected devices such as: gain, bandwidth, antenna radiation diagrams or physical parameters for the synthesis of antennas or frequency selective surfaces (FSS). Hence, hybrid optimization solutions are developed – among which the cuckoo search (CS) algorithm proposed by Yang and Deb deserves to be highlighted [6].

By exploring the potential of these computational tools, researchers plan ANNs to work paired to optimization algorithms, thus creating the so-called hybrid methods [3, 4, 7–9]. That is, after training with numerically calculated electromagnetic (EM) data, the ANN generates a search space denominated as the region of interest (ROI), in which optimization algorithms look for the best solutions, i.e. the ones that can attend to a designated objective function (or cost function). This process allows greater flexibility and robustness to the project, warranting more precise results and, in some cases, substantially minimizing the demanded processing time for EM properties calculations. Such qualities are the main cause for the employment of these techniques in microwave applications [10].

In the states of art there is a vast literature with the most diversified projects of FSSs for application in microwaves. In [11], e.g., the authors proposed a three-layer broadband FSS for applications in that system, however, many iterations were necessary to achieve satisfactory geometric shapes in each of the three layers, and thus to achieve operation in broadband, the BIC could have helped.

In this context, the authors in [12] proposed a double-sided broadband FSS - approximately 4GHz - for operation in the X band. However, the design of the structure is too complex, due to the geometric shape

of the unit cell that resembles a fractal, the substrate of the device is made of filaments that form a metallic grid and no optimization process has been proposed to enable the optimization of the design steps.

As at [13] a wide-band frequency FSS based on double-layered hexagonal unit cell was presented. The project also requires several interactions until the desired geometric shape is achieved in each of the unit cell of the layers, making it difficult to reproduce the filter by people interested in the work, and no automatic optimization process is presented to overcome this difficulty.

The proposed geometry of the FSS presented in [14] consists of a square loop and a triangle conductor which are etched to a single layer dielectric substrate, for X and Ku bands applications. Several geometric parameters had to be adjusted in the project to achieve a satisfactory result, which can generate excessive time for the calculation of the EM properties of the device, as well as high effort because it is a trial-and-error method.

FSS can be employed, for example, to make the antenna reflector more efficient [15–20]: reducing reflections and undesirable radiations; by adjust the wave polarization and propagation, as well as bandwidth control; and allowing the simultaneous application of more than one source in the same reflector. As previously explored, although discussed works presents satisfactory results, there are some difficulties to be overcome if any person interested in the project wishes to reproduce it, either by the complexity of the geometries of the unit cells presented, or by the high number of iterations required. A viable solution would be to introduce some automatic process to obtain the desired parameters – e.g., through some computational intelligence technique or by the use of BIC optimization techniques – i.e., the trial and error method would be easily overcome, which would result in a drastic reduction in the time required for the project conclusion, as well as would avoid failures that may occur throughout the process because once the calculations of the EM properties of the device, these would feed the processing applied for data processing and the geometric parameters would be calculated according to the objectives configured in the cost function, as desired in the project.

With this in mind, two multiobjective hybrid BIC techniques are presented in this study for the design and synthesis of a of a multilayer FSS of simplified geometry unit cell and low-cost manufacturing. The objectives for the optimization process are the control of lower and upper cutoff frequencies that limit the operational bandwidth of the devices, which are in turn set to the reference threshold of -10 dB. A reduction of optimization and processing time of calculated EM data is also desired. Furthermore, after the optimization and synthesis of said FSSs, angular stability tests have been executed for angles: 10° , 20° and 30° and 40° , as well as proof of independence of incident wave polarization. It has been verified that the devices herein presented denote good angular stability and polarization independence.

This paper is structured as such: Section 2 discusses details about the design of the FSSs. Section 3 details the employed BIC techniques. In Section 4, the hybrid method proposed by the authors is further discussed. Section 5 displays the study's results and in Section 6 conclusions are discussed.

2. Patch-type FSS Design

Frequency selective frequencies (FSSs) are planar and periodical structures composed by metallic components of either slot or patch type, capable of reflecting (bandstop) or transmitting (bandpass)

electromagnetic waves in frequencies that are proximate to the device's resonance [21]. These periodic arrays behave similarly to radiofrequency circuit filters [22]. The influence exerted by physical parameters such as the substrate's depth, permittivity and isotropic behavior is observed in the bandwidth and resonance characteristics of an FSS [23, 24].

In this study the design of a double-layer FSS separated by an air gap is discussed, in which the first layer's unit cell conductors are triangular loops and the second layer ones are solid lozenges, inspired by the usage presented in [7] and [3] respectively. A schematic of the structure is displayed in Figure 1.

In computational simulations, the FSS have been considered as printed in glass epoxy substrate (FR-4), possessing relative permittivity of

3. Bioinspired Computing

Bioinspired computing (BIC) is an important tool in Computer Science, in which techniques based on Biology and behavior of living beings are then transcribed into coding. Such techniques have been successfully modeled over the years, being capable of solving complex general problems related to optimization in engineering and industry [5].

The proposed hybrid technique, applied to optimize the devices shown in this study, includes a general regression neural network (GRNN) [25] combined with the multiobjective genetic algorithm (MOGA) [8] and the multiobjective cuckoo search (MOCS) [26]. The FSSs have been designed to possess simplified and low-cost geometries, in order to obtain two bandstop filters: the first filter is applied to the X band (8 – 12 GHz) and the second one to C and Ku bands (4 – 8 GHz and 12 – 18 GHz, respectively).

The following sections present greater detail on BIC techniques developed in this paper.

Despite being remodeled in 1991 by B. Specht [25] to realize general regressions (be it linear or non-linear), the concept of a GRNN was first introduced in 1964 by Nadaraya [27] and Watson [28]. It is a type of Radial Base Neural Network (RBNN), based on non-parametric estimation and advantageous in needing only a small part of the database to conduct the network's training. Likewise, it has the capacity to rapidly converge to a satisfactory data function, making retropropagation unnecessary – also turning itself into a useful tool for system performance prediction and / or comparison [7].

Figure 2 presents the developed network's schematic.

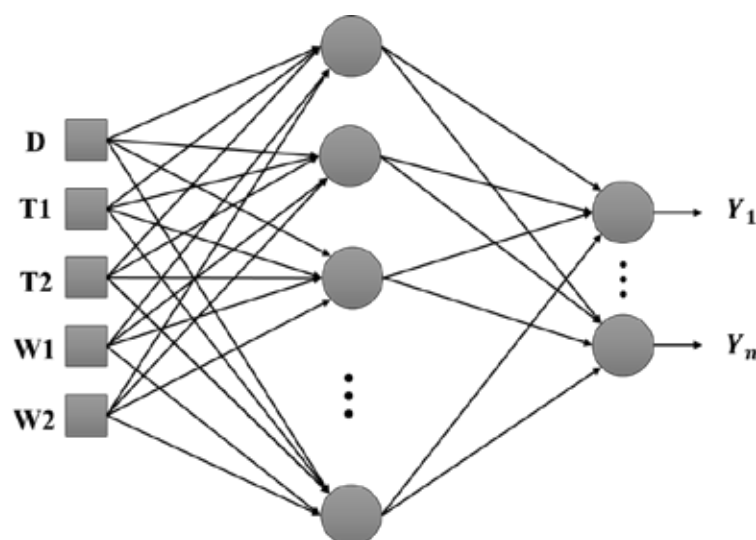


Figure 2. Configuração da GRNN utilizada.

A GRNN has been created herein carrying five inputs and two outputs, according to the specifications for the formation of the ROI. That said, the network recognizes the patterns of the samples inserted into their inputs at the moment of the training. Thus, the number of intermediate layer (also called “hidden layer”) neurons varies according to the number of data utilized at the learning phase.

The inputs and outputs of the GRNN can be represented by vectors, keeping in mind that the outputs differ according to the filter that is analyzed. Therefore, the entrances for both filters are to be represented as:

(1)

in which D is the distance between plates, T_1 is the periodicity of plate 1, T_2 is the periodicity of plate 2, W_1 is the unit cell conductor dimension on plate 1 and W_2 is the unit cell conductor dimension on plate 2. For the first filter, the output is represented by:

(2)

where LCF is the lower cutoff frequency and UCF stands for the upper cutoff frequency in filter 1.

For the second filter, the output is:

(3)

where UCF1 is the upper cutoff frequency for band 1 and LCF2 is the lower cutoff frequency for band 2 in filter 2.

Genetic algorithms (GAs) are natural selection and genetic-based search procedures, with applicability in general optimization problems and, particularly, in automatic learning. This algorithm was introduced by Holland [29] in 1975 and popularized by his pupil Goldberg [30] in 1989. They follow the principles of “survival of the fittest” and natural selectivity as declared in 1859 by the biologist and physiologist Charles Darwin in his book “The Origin of the Species”. Holland was the first researcher to utilize the concepts of selection, crossover and mutation in the study of artificial adaptive systems [29].

GAs belong to the stochastic, natural selection algorithm category [31, 32], operating with a population of candidate solutions to satisfy mono or multiobjective criteria. These solutions go through operator with the intent of keeping the populational variability and are analyzed by selections that evaluate the better-adapted individuals in a given environment – that is, the problem’s search space [33, 34].

In this work, the implemented technique is based on the non-dominated sorting genetic algorithm II (NSGA II), as it differs from its counterparts by the manner in which the fittest chromosome is selected. During the selection stage, the algorithm classifies the total population in fronts, according to the degree of dominance, and the individuals who reside in the first front are considered the best solutions of that generation, while the ones at the last front are considered the worst [35].

According to this premise, it is possible to find results that are better suited to the problem in question. Some important aspects in multiobjective problem-solving are:

- Divide the population in different levels (or fronts) with the aid of a dominance criterion;
- The front individuals are better than the ones in front $+ 1$;

In this manner, the algorithm classifies the total population in different quality categories by employing a dominance criterion, permitting the prioritization of those amongst the better classified. NSGA II’s operation is peculiar for possessing two important mechanisms in the selection process, which are: 1) non-dominated sorting (NDS) and 2) crowding distance (CD).

The concept of dominance is given by P and Q , which are considered same-population individuals, however P dominates Q in case P does not have any objectives with an inferior quality than Q . That way, initially, there is a non-classified population that shall go through an attribution process with a dominance degree

given to each individual in relation to all of the others in the total population. After this step, they are placed in fronts, and the best individuals are allocated in the first front, as previously said.

After going through the NDS process, the population is to be classified by the density operator, that is, the CD mechanism, aiming to order each individual in relation to its distance to other neighbor dots within the same front (for each objective). Hence, the more distant to the central dot the greater is the probability of being chosen, allowing for better scattering of results along the front and avoiding solution clustering over the same dot. The next steps are the crossover and mutation processes, which are identical to a conventional GA.

Figure 3 presents a multiobjective GA operation flowchart.

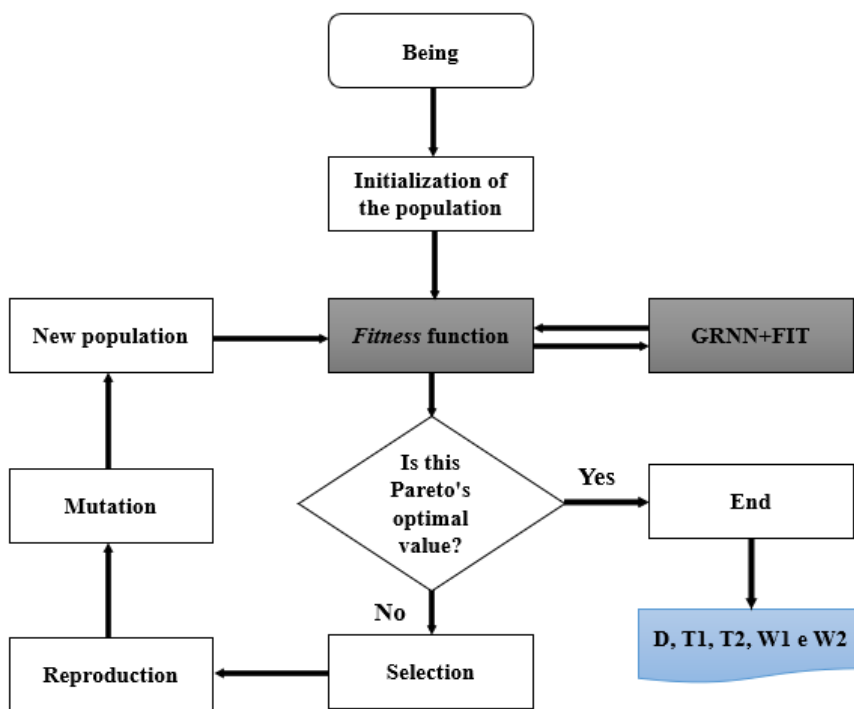


Figure 3. Operation flowchart of a multiobjective GA.

One of the most recent nature-inspired metaheuristic algorithms, the Cuckoo Search (CS) is part of the swarm intelligence algorithm group and was first proposed by Yang and Deb in 2009 [6]. Its applications aim at solving multimodal problems, and its biological inspiration is based on an interesting and aggressive characteristic of reproduction of some species of cuckoos – the so-called nest parasitism.

There are two basic types of parasitism: intraspecific nesting, cooperative reproduction and nest acquisition. Generally, cuckoos choose a nest where the host Bird has already deposited its own eggs. Given that the cuckoo's eggs hatch faster, once the parasite hatchling leaves the eggshell it instinctively throws the other eggs away from the nest, thus augmenting its participation in the quantity of nourishment provided by the host bird. In addition, some hatchlings can also imitate the call pattern of the host to gain access to feeding. Sometimes, optimization problems involve more than a single objective. Therefore, by utilizing the

multiobjective cuckoo search (MOCS) in multiple objectives, there is a need to alter the first and last rules of the original CS code in order to incorporate multiobjective operation [36]:

- Each cuckoo lays eggs at a time, putting them in a randomly chosen nest. The egg corresponds to the solution of the i -th objective;
- The best nests with high-quality eggs (solutions) are chosen to be carried on into future iterations;
- The number of available nests is constant and the host bird may discover an “alien” cuckoo egg with a probability of $p_a \in [0,1]$. In this case, the host bird can get rid of the egg or abandon the nest altogether to build another one in a new spot.

For the last rule, it is presumed that instead of a fraction of nests be abandoned, they are outright substituted by novel nests (containing new random solutions in another place within the search space).

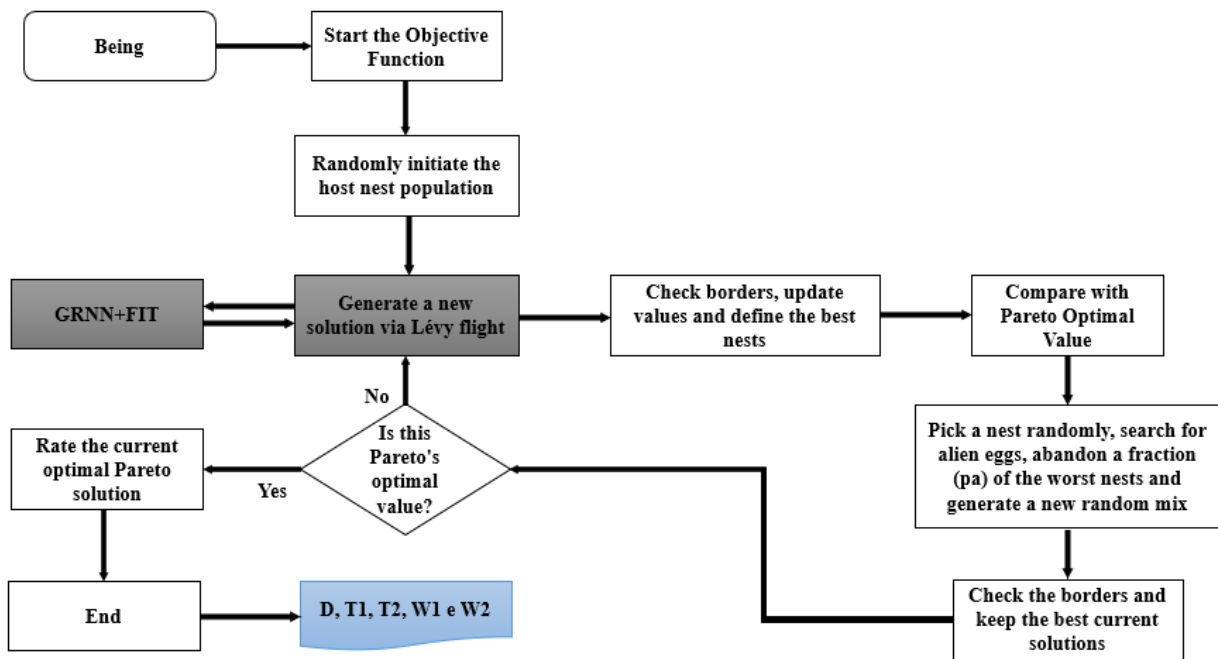


Figure 4. Multiobjective cuckoo search (MOCS) algorithm flowchart.

Figure 4 presents a flowchart covering the functioning principles of MOCS. The algorithm is composed, structurally, by two main operations. One is a direct search based on Lévy Flights [6], and the second is a random search based on the host bird’s probability of finding in its nest an “alien” egg. Just as in other metaheuristic populational algorithms, MOCS utilizes population elitism in order to find an optimal solution to the outputs – in this case, each nest is considered a different solution.

4. Hybrid Optimization Technique

The objective of the implemented optimization algorithms is to minimize the cost function and synthesize the proposed filters, and can be defined as [4, 7—9]:

$$(4)$$

in which Δ and δ represent the difference between results given by the GRNN and the values

specified at the cost function.

The ideal solution is to find values that would turn the variables of the cost function into zero or very proximate to it. However, in non-convex problems, the function’s values may not converge to a null figure. Therefore, a Pareto front is created containing non-dominated solutions, generating a set of solutions that are not strictly dominated in each iteration.

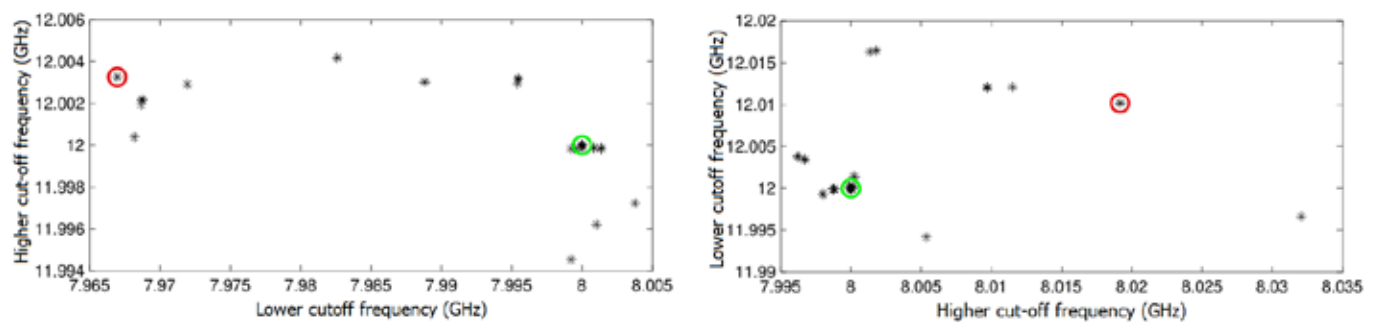
For the relation of dominance, if R dominates S when R is a region of viable solutions that, e.g., dominates S if R is considered partially greater or greater than S , that is:

$$(5)$$

and

$$(6)$$

In case no R exerts dominance over S , so S is assumed to be the optimal Pareto solution. Figure 5 presents the relation of dominance, for one iteration, of both filters investigated in this study. The asterisk markers are the best responses that satisfy the objectives for each filter along the Pareto front during the algorithm’s execution. Furthermore, the red circular markers represent the worst (dominated) solution and the green ones denote the best solutions (non-dominated).



(a) Filter 1.

(b) Filter 2.

Figure 5. The Pareto front.

After calculations of the EM properties of the structures by the FIT complete-wave technique, by varying the structural parameters of proposed devices (see Table 1), the hybrid techniques GRNN+MOGA and GRNN+MOCS have been applied to substitute the necessity of new computation simulations and, thus, minimizing computational cost. Along the simulations, it is possible to perceive that little variations in the parameters of the FSS result in greater in the frequency response, so rendering necessary a greater refinement in parameter variation, elevating the computational costs even more.

With this impasse in mind, the optimal values localized at the Pareto front are assumed as reference points to the creation of a new dataset, utilizing a lesser step size of each of the analyzed parameters. Thus, it is possible to make mappings at the ROI only taking into consideration values that can fulfill the specified objectives for each filter – and this is purpose of the proposed optimization algorithms.

Table 2 present optimal values for both filters according to the developed hybrid techniques.

Table 2. Structural parameters for the multilayer FSS

Filter	Hybrid Technique	Parameters				
		D	T1	T2	W1	W2
1	GRNN – AG Multi	3.3804	12.8741	13.7894	9.7615	12.8668
	GRNN – MOCS	2.5	13.8160	14.3130	9.5108	13.3630
2	GRNN – AG Multi	2.5	14.7502	12.1658	13.3905	9.2197
	GRNN – MOCS	2.5719	14.1448	12.2795	13.8515	9.1425

Cutoff frequency values for the control of bandwidth have been obtained at the threshold of -10dB. Numerical validation of results has been made by FEM calculations, with the aid of software Ansoft HFSS. Percentual deviation, relative to FIT-calculated results compared to FEM-calculated ones, are defined as such:

$$\text{Dev} = \frac{|O_{sim} - O_{fit}|}{O_{fit}} \times 100 \tag{7}$$

in which O_{sim} is the value of the simulation-returned objective according to optimized parameters, O_{fit} is the objective value and O_{an} are the analyzed objectives.

Figure 6 shows fitness evolution in the synthesis process through multiobjective GA for filter 1. Along the iterations, the cost function value gradually diminishes, in which the dotted line represents the fitness average for the the cromossome population and the solid line represents the average of best individual solutions. A population of 100 cromossomes had been considered, and the number of elite cromossomes was limited to a fraction of 0.25 of the Pareto front. A total of 102 iterations and, approximately, 110.076 seconds were necessary for optimization convergence.

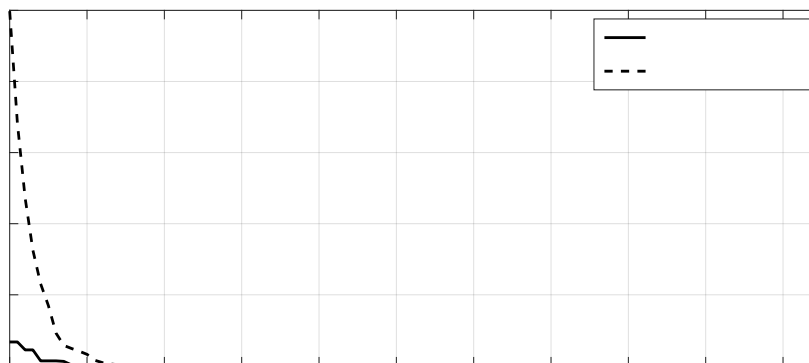


Figure 6. Fitness evolution of the multilayer FSS synthetic process for filter 1 via MOGA.

Figure 7 displays fitness evolution of the synthesis through multiobjective GA for filter 2. In this case, it has been considered a population of 75 cromossomes, and the number of elite cromossomes has also been limited to a fraction of 0.25 of the Pareto front, for a total of 322 iterations and 306.796 seconds for the code to converge.

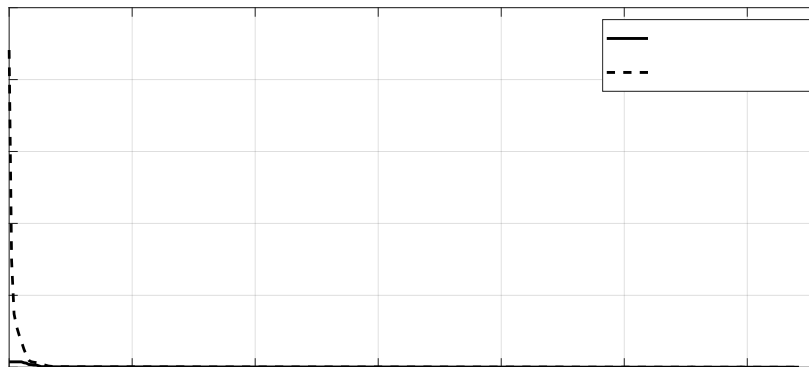


Figure 7. Fitness evolution of the multilayer FSS synthetic process for filter 2 via MOGA.

Figure 8 shows fitness evolution this time through MOCS for filter 1. A set of 100 nests and probability = 0.25 has been utilized, with scalar vector The code has converged in around 500 iterations and approximately 1181.159 seconds.

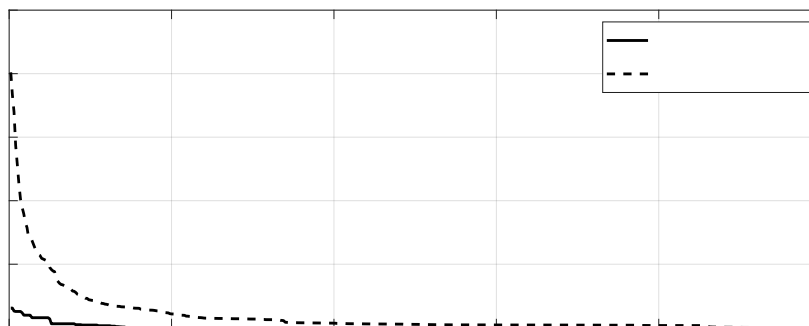


Figure 8. Fitness evolution of the multilayer FSS synthetic process for filter 1 via MOCS.

Figure 9 shows fitness evolution this time through MOCS for filter 2. A set of 100 nests and probability = 0.75 has been utilized, with scalar vector The code has converged in around 500 iterations and approximately 1198.346 seconds.

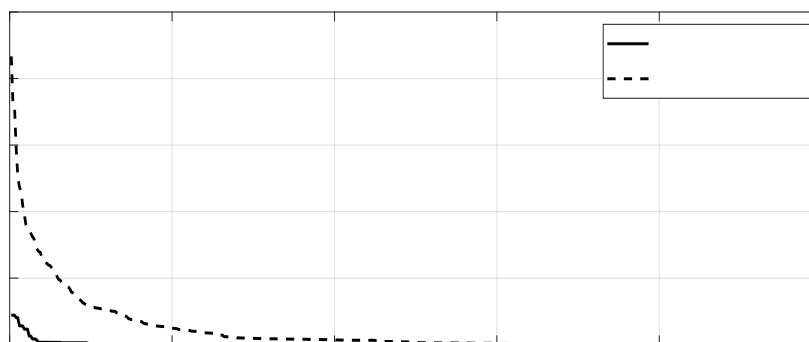


Figure 9. Fitness evolution of the multilayer FSS synthetic process for filter 2 via MOCS.

5. Results

For filter 1, the proposed GRNN contains 5 first-layer entrances, an intermediate layer containing 768 neurons and 2 exit nodes representing the lower and upper cutoff frequencies. Table 3 displays the structural parameters, as well as input data for the learning and training of the GRNN.

Table 3. Structural parameters for filter 1

Parameters	Values
Distance between plates, D (mm)	[2, 2.5, 3, 3.5]
Periodicity of plate 1, T1 = Tx1 = Ty1 (mm)	[12.5, 13, 13.5, 14]
Periodicity of plate 2, T2 = Tx2 = Ty2 (mm)	[14.5, 15, 15.5]
Conductor element dimensions on plate 1, W1 = Wx1 = Wy1 (mm)	[9, 9.5, 10, 10.5]
Conductor element dimensions on plate 2, W2 = Wx2 = Wy2 (mm)	[12.5, 13, 13.5, 14]

Figure 10 presents results for the transmission coefficient calculated via FIT and FEM utilized for result validity. The applied hybrid technique consists of a GRNN+MOGA configuration. The obtained optimal parameters are D = 3.0682 mm; T1 = 13.7336 mm; T2 = 15.3977 mm; W1 = 9.92 mm and W2 = 13.7594 mm.

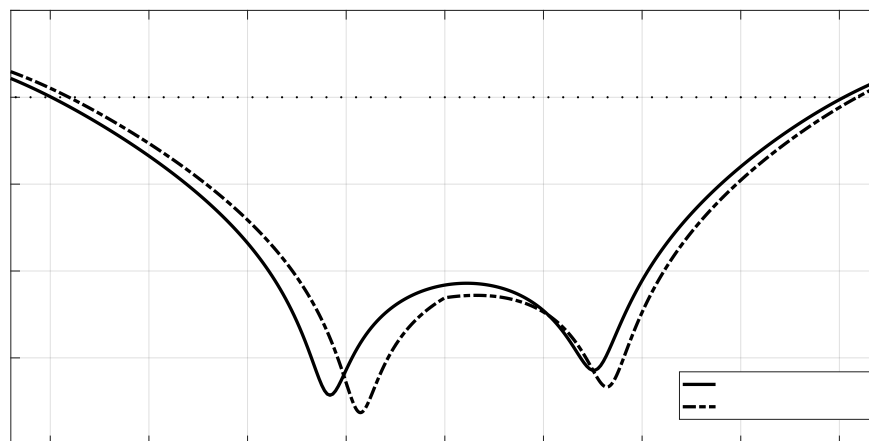


Figure 10. Transmission coefficient of the multilayer FSS for filter 1 via MOGA.

The objectives for the filter were set as 1: 1) lower cutoff frequency at 8 GHz, and 2) upper cutoff frequency at 12 GHz. With this, the frequencies belonging to the X band are rejected and the transmission of the frequencies belonging to the band C (4 - 8 GHz) is made possible, as well as the Ku band (12 -18 GHz). When analyzing the results presented in Figure 10, it is observed that the values obtained in relation to the lower cutoff frequency and the upper cutoff frequency are, respectively, 8,005 GHz and 12,023 GHz for results calculated by FIT, which represents a relative error in relation to the configured objectives in the BIC code of about 0.25%. Then, when verifying results calculated by FEM, the values obtained for the lower frequency and the upper cutoff frequency were, respectively, 8,095 GHz and 12.09 GHz, which

corresponds to a relative error of 1.94% regarding the objectives of BIC.

Figure 11 presents the results for the transmission coefficient referring to the multilayer FSS corresponding to filter 1. These results were calculated from the optimal structural parameters returned by the hybrid technique GRNN + MOCS, consisting of the following values: $D = 3.2433$ mm, $T1 = 13,893$ mm, $T2 = 15.2829$ mm, $W1 = 9.9828$ mm, and $W2 = 13.5089$ mm.

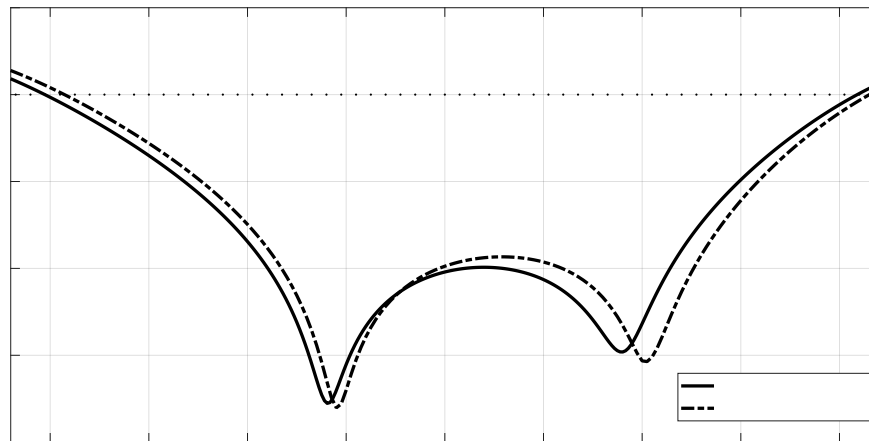


Figure 11. Transmission Coefficient for Multilayer FSS of filter 1 via MOCS.

When analyzing the results presented in Figure 11, it is observed that the values obtained in relation to the lower cutoff frequency and the upper cutoff frequency are, respectively, 7,971 GHz and 12,091 GHz for results calculated from FIT, in which represents a relative error in relation to the objectives configured in the BIC code of around 1.12%. Then, when verifying the result calculated by the FEM method, the values obtained for the lower cutoff frequency and the upper cutoff frequency were, respectively, 8,075 GHz and 12.15 GHz, which corresponds to a relative error of 2.19% in relation to the objectives of BIC.

Regarding filter 2, the developed GRNN contains 5 inputs in the first layer, an intermediate layer containing 216 neurons and two output nodes referring to the upper cutoff frequency of the first band and the lower cutoff frequency of the second band, which sets up the device as dual-band. Table 4 presents the structural parameters and values for filter 2, which were inserted unto the GRNN training and learning entries.

Table 4. Parâmetros Estruturais das FSS Multicamadas para o Filtro 2

Parâmetros	Valores
Distância entre as placas, D (mm)	[1.5, 2, 2.5, 3]
Periodicidade da placa 1, $T1 = Tx1 = Ty1$ (mm)	[14, 14.5]
Periodicidade da placa 2, $T2 = Tx2 = Ty2$ (mm)	[11.5, 12, 12.5]
Dimensões do elemento condutor da placa 1, $W1 = Wx1 = Wy1$ (mm)	[12.5, 13, 13.5]
Dimensões do elemento condutor da placa 2, $W2 = Wx2 = Wy2$ (mm)	[8.5, 9, 9.5]

Figure 12 denotes the results for the transmission coefficient calculated via FIT versus calculated via FEM. For this optimization the hybrid technique GRNN + MOGA was used, considering the multilayer FSS

referring to filter 2. The optimal structural parameters obtained were $D = 2.1068$ mm, $T1 = 14.4721$ mm, $T2 = 12.2558$ mm, $W1 = 13.1044$ mm, and $W2 = 8.9673$ mm.

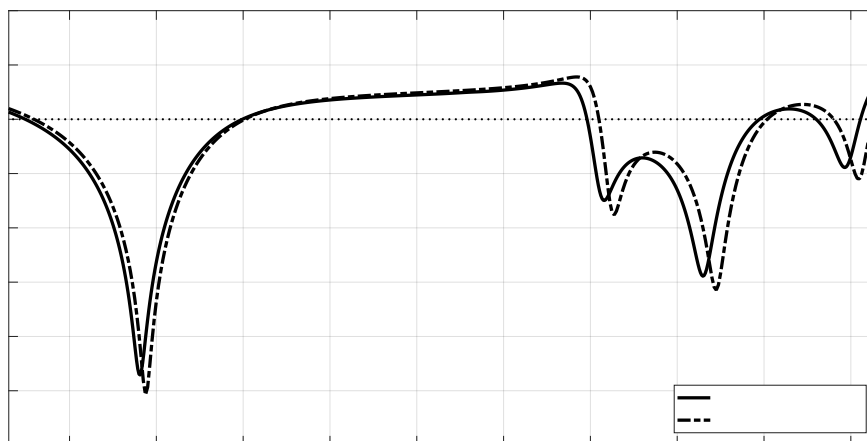


Figure 12. Transmission Coefficient for Multilayer FSS of filter 2 via MOGA.

The objectives of filter 2 are to tune the upper cutoff frequency for the first operating band at 8 GHz, and the lower cutoff frequency for the second operating band at 12 GHz. With this, the X band is transmitted and the C and Ku bands are blocked, which also characterizes the device as dual-band.

Still according to Figure 12, it is observed that the values obtained concerning the lower cutoff frequency and the upper cutoff frequency are, respectively, 7,995 GHz and 11,961 GHz for the result calculated from the FIT, which represents a relative error in relation to the objectives configured in the BIC code of about 0.39%. Then, when verifying the result calculated by FEM, the values obtained for the lower cutoff frequency and the higher cutoff frequency were, respectively, 8.02 GHz and 12.1 GHz, corresponding to a relative error of 1.08% to the objectives of BIC.

Figure 13 presents the results for the transmission coefficient calculated via FIT versus the calculated via FEM, when considering the optimal structural parameters returned by the hybrid technique GRNN + MOCS for the multilayer FSS referring to filter 2. The optimal parameters obtained were $D = 1.7845$ mm, $T1 = 14.5$ mm, $T2 = 12.3419$ mm, $W1 = 12.9119$ mm, and $W2 = 8.785$ mm.

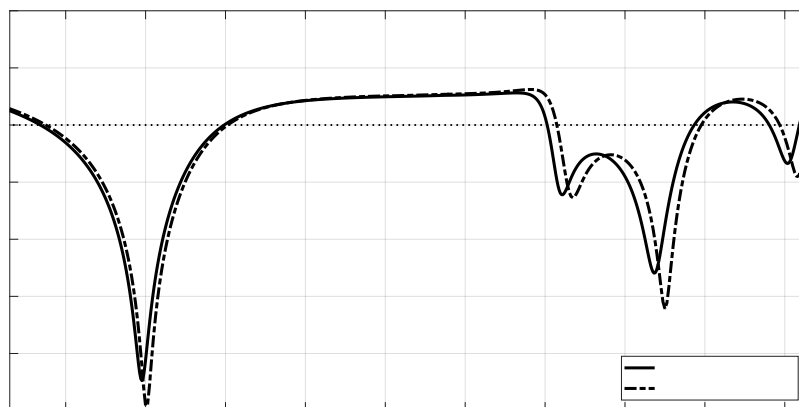
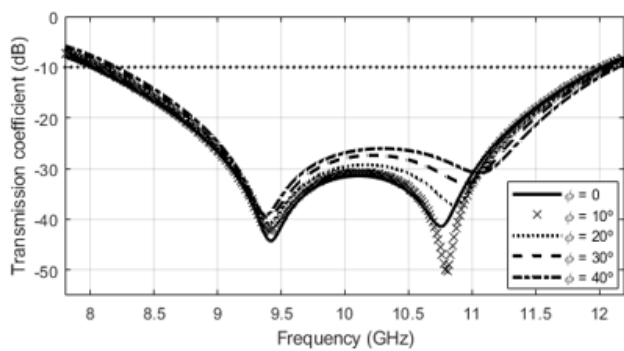


Figure 13. Transmission Coefficient for the Multilayer FSS of filter 2 via MOCS.

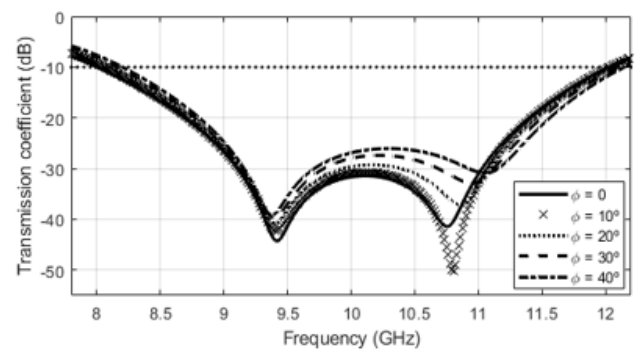
When analyzing the results presented in Figure 13, it can be noted that the values obtained in relation to the lower cutoff frequency and the upper cutoff frequency are, respectively, 7,983 GHz and 12,026 GHz, for the result calculated from FIT, the which represents a relative error in relation to the objectives configured in the BIC code of about 0.43%. Then, when verifying the result calculated by FEM, values for the lower cutoff frequency and the upper cutoff frequency were, respectively, 8,025 GHz and 12.15 GHz, which is equal to a relative error of 1,562% in relation to the objectives of BIC.

A characteristic that must be taken into account when analyzing FSS, be it single layer or multilayer, is the angular stability of the device, given that this aspect allows the analysis of the capacity that the FSS has to operate effectively in the filtering of electromagnetic waves with oblique incidence coming from multiple paths. However, an evaluation of FSS response for the two main types of polarization, horizontal and vertical, should be considered.

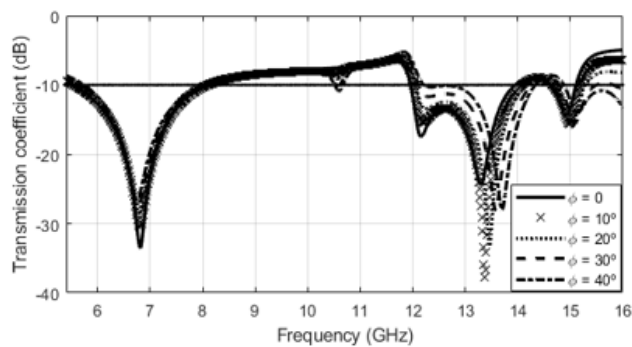
The angular phase stability calculated from FIT is shown in Figure 13 for both filters optimized via MOGA. These results were considered because this technique has shown a higher degree of precision in meeting the project’s objectives.



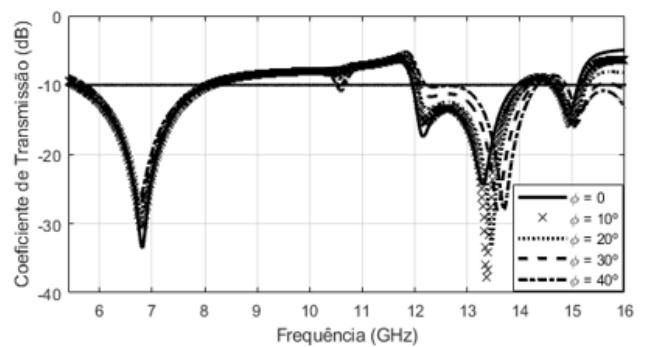
(a) Filter 1 – TM polarization.



(b) Filter 1 – TE polarization.



(c) Filter 2 – TM polarization.



(d) Filter 2 – TE polarization.

Figure 14. Angular stability of filters 1 and 2 for horizontal and vertical polarizations.

Figures 14 (a) and (c) show the calculated results for filter 1, while Figures 14 (b) and (d) show the calculated results for filter 2. When analyzing these results, it is verified that the behavior of the devices

remains unchanged regardless of the incident wave polarization, confirming that the multilayer FSS are independent of the incident wave polarization. According to the consensus found in the literature, the proposed FSS is characterized as having an independent polarization.

With regard to angular stability, specifically in Figures 14 (a) and 14 (b), it is noteworthy that for the incidence angle of 40° the lower and upper cutoff frequencies have a deviation of approximately 160 MHz and 75 MHz, respectively, in relation to the normal incidence angle. As the application of filter 1 consists of a rejection of X band frequencies, these values of deviation in the cutoff frequencies meet the prerequisite of a maximum deviation of 2% in relation to the normal incidence wave. This ensures that the device operates with good angular phase stability for waves with an oblique incidence of up to 40°.

For Figures 14 (c) and 14 (d), when analyzing the critical angle of incidence of 40°, the lower and upper cutoff frequencies for the first rejection band show deviations of about 147 and 140 MHz, respectively, in normal incidence angle. However, it is observed that the frequencies belonging to the Ku band (12–18 GHz) suffer greater distortions when subjected to different angles of wave incidence, which can be justified by the wavelength being shorter for this band – which makes it more sensitive to these variations and fatally contributes to the formation of reflected waves between filter plates with phases that cancel each other out, thereby distorting the frequency response of the device. However, for the first rejection band, the deviation values at the cutoff frequencies meet the prerequisite for a maximum deviation of 2% with respect to the normal incidence wave.

Table 5 presents a summary of the synthesis process of the filters designed in this work.

Table 5. Summary of obtained data

Filter 1							
Hybrid Technique	Iteration Count	Convergence Time (in seconds)	Numerical Technique	Objectives		Error (%)	Angular Stability
				LCF1 (8 GHz)	UCF1 (12 GHz)		
GRNN + MOGA	102	110.037	FIT	8.005	12.023	0.254	Up to 40°
			FEM	8.095	12.09	1.937	
GRNN + MOCS	500	1181.159	FIT	7.971	12.091	1.121	
			FEM	8.075	12.15	2.187	
Filtro 2							
Hybrid Technique	Iteration Count	Convergence Time (in seconds)	Numerical Technique	Objectives		Error (%)	Angular Stability
				LCF1 (8 GHz)	UCF2 (12 GHz)		
GRNN + MOGA	322	306.796	FIT	7.995	11.961	0.387	Up to 40°
			FEM	8.02	12.11	1.083	
GRNN + MOCS	500	1198.396	FIT	7.983	12.026	0.429	
			FEM	8.025	12.15	1.562	

6. Conclusion

This study discussed two BIC techniques that combine GRNN with the optimization algorithms MOGA and MOCS, respectively, applied in the design of multilayer FSSs. The calculation of the electromagnetic properties of the proposed devices was performed using the FIT numerical technique, and the computational results were validated by the FEM numerical technique.

The hybrid techniques proved to be fast and accurate. However, when confronted, the technique that combines GRNN + MOGA proved to be superior to GRNN + MOCS. The precision and speed in the convergence of MOGA can be attributed to the fact that the code's heuristic process is metapopulation, which makes the optimization process intuitive, especially when the number of parameters to be optimized is relatively large, since operations that occur during the optimization guarantee high variability among the possible solutions for the objective function of the problem.

The proposed devices were also subjected to independent polarization tests of incident-wave in TE and TM, as well as an angular phase stability test for both filters. Both multilayer FSSs were independent of the incident-wave polarization. However, only filter 1 showed good angular stability up to the critical angle of 40° for the entire operating range of the filter. Whereas filter 2, which has a dual-band filtering operation, proves stable up to the critical angle of 40° for the first filtering band in band C, however, the results for the frequencies of the second operating band, band Ku, were not satisfactory regarding the deviation criterion employed of about 2% in relation to the normal incidence in the plane of the structure. The geometries of the unit cells that make up the multilayer FSSs were chosen due to the geometric simplicity and the ease of reproducing the models, as shown in Figure 1.

Finally, it is noteworthy that in the state of the art GRNN-type networks, as well as hybrid techniques, had only been employed in the single layer FSS optimization process – this being another contribution of this study, i.e., the applicability of the proposed hybrid techniques in the design and synthesis of an asymmetric multilayer FSSs.

7. References

- [1] A.H. Alavi, and A.H. Gandomi, “A robust data mining approach for formulation of geotechnical engineering systems”, *International Journal of Computer Aided Methods in Engineering-Engineering Computations*, vol. 28, no. 3, 2011, pp. 242–74.
- [2] S. Ali, N. Abbadeni, M. Batouche, “Multidisciplinary computational intelligence techniques: applications in business, engineering, and medicine”, IGI Global Snippet, 2012.
- [3] M.C. Alcantara Neto, H.R.O. Ferreira, J.P.L. Araujo, F.J.B. Barros, A. Gomes Neto, M.O. Alencar, G.P.S. Cavalcante, “Compact ultra-wideband FSS optimised through fast and accurate hybrid bio-inspired multiobjective technique”, *IET Microwaves, Antennas & Propagation*, 2020, pp.1-9.
- [4] M.C. Alcantara Neto, J.P.L. Araujo, R.J.S. Mota, F.J.B. Barros, F.H. Ferreira, G.P.S. Cavalcante, B.C. Lyra, “Design and Synthesis of an Ultra Wide Band FSS for mm-Wave Application via General Regression

Neural Network and Multiobjective Bat Algorithm”, *Journal of Microwaves, Optoelectronics and Electromagnetic Applications*, 18, (4), 2019, pp. 530-544.

[5] Z. Cui, R. Alex, R. Akerkar, X.S. Yang, “Recent advances on bioinspired computation”, *The Scientific World Journal*, 2014, pp. 1-3.

[6] X.S. Yang, and S. Deb, “Cuckoo search via Lévy flights”, in: *Proc. of World Congress on Nature & Biologically Inspired Computing (NaBic 2009)*, IEEE Publications, 2009, USA, pp. 2010-2014.

[7] M.C. Alcantara Neto, J.P.L. Araujo, F.J.B. Barros, A.N. Silva, G.P.S. Cavalcante, A.G. D’Assuncao, “Bioinspired multiobjective synthesis of x-band FSS via general regression neural network and cuckoo search algorithm”, *Microwave and Optical Technology Letters*, 57, (10), 2015, pp. 2400-2405.

[8] M.C. Alcântara Neto, F.J.B. Barros, J.P.L. Araújo, H.S. Gomes, G.P.S. Cavalcante, A.G. d’Assunção, “A metaheuristic hybrid optimization technique for designing broadband FSS”, *SBMO/IEEE MTT-S Int. Microwave and Optoelectronics Conference (IMOC)*, Porto de Galinhas, Brazil, November 2015, pp. 3-6.

[9] W.C. Araújo, H.W.C. Lins, A.G. d’Assunção Jr, J.L.G. Medeiros, A.G. d’Assunção, “A bioinspired hybrid optimization algorithm for designing broadband frequency selective surfaces”, *Microwave and Optical Technology Letters*, 56, (2), 2013, pp. 329–333.

[10] A. Hoorfar, “Evolutionary programming in electromagnetic optimization: a review”, *IEEE Trans. Antenna and Propagation*, 2007, pp. 523–537.

[11] S. Can, A.E Yilmaz, “Bandwidth enhancement of a triangle with gridded-square loop-loaded FSS for X and Ku bands”, *IEEE The 8th European Conference on Antennas and Propagation (EuCAP)*, The Hague, Netherlands, 2014, pp. 6–11.

[12] A. Chatterjee, B. Mandal, S.K. Parui, “A FSS Based Corner Reflector for Performance Enhancement of a Ribcage Dipole Antenna”, *IEEE Applied Electromagnetics Conference (AEMC)*, Guwahati, India, 2015, n. 16142482.

[13] C.C. Hunag, N.W. Chen, “Frequency Selective Surface for Reflector Antenna with Multiple Feeds”, *IEEE International Symposium on Antennas and Propagation*, Chicago, IL, USA, 2012, n. 13134982.

[14] M. Yan, J. Wang, S. Qu, M. Feng, Z. Li, H. Chen, J. Zhang, L. Zheng, “Highly-selective, closely-spaced, dual-band FSS with second-order characteristic”, *IET Microwaves, Antennas & Propagation*, 2016, 10, (10), pp. 1087-1091.

[15] K. Ding, C. Gao, T. Yu, D. Qu, “Wideband CP slot antenna with backed FSS reflector”, *IET*

Microwaves, Antennas & Propagation, 2017, 11, (7), pp. 1045-1050.

[16] M. Yan, J. Wang, H. Ma, S. Qu, J. Zhang, C. Xu, L. Zheng, A. Zhang, "A Quad-Band Frequency Selective Surface With Highly Selective Characteristics", *IEEE Microwave and Wireless Components Letters*, 2016, 26, (8), pp. 562–564.

[17] K. Bencherif, M. Titaouine, R. Saidi, A. Djouimaa, I. Adoui, T.R. Sousa, A. Gomes Neto, H. Baudrand, "Multiband FSS analysis and synthesis based on parallel non coupled metallic strips using WCIP method", *Journal of Microwaves, Optoelectronics and Electromagnetic Applications*, 2018, 17, (4), pp. 433-456.

[18] J. Zhu, Y. Yang, S. Li, S. Liao, Q. Xue, "Dual-Band Dual Circularly Polarized Antenna Array Using FSS-Integrated Polarization Rotation AMC Ground for Vehicle Satellite Communications", *IEEE Transactions on Vehicular Technology*, 2019, 68, (11), pp. 10742-10751.

[19] G.H. Schenum, "Frequency-selective surfaces for multiple frequency antennas", *Microwave Journal*, 1973, v. 16, n.5, p. 55-57.

[20] P.H.F. Silva, A.F. Santos, R.M.S. Cruz, A.G. D'Assunção, "Dual-band bandstop frequency selective surfaces with gasper prefractal elements", *Microwave and Optical Technology Letters*, 2012, 54, (3), pp. 771-775.

[21] Munk, B. A., "Frequency Selective Surfaces: Theory and Design", [S.l.]: John Wiley & Sons, Inc., 2000.

[22] M. Lambea, M.A. Gonzalez, J.A. Encinar, J. Zapata, "Analysis of frequency selective surfaces with arbitrarily shaped apertures by finite element method and generalized scattering matrix", *IEEE Antennas and Propagation Society International Symposium*. [S.l.]: IEEE, v. 4, 1995, p. 1644–1647.

[23] A.C.C. Lima, E.A. Parker, and R.J. Langley, "Tunable frequency selective surface using liquid substrates", *Electronics Letters, Institution of Engineering and Technology (IET)*, v. 30, n. 4, 1994, p. 281–282.

[24] Y.G. Li, Y.C. Chan, T.S. Mok, J.C. Vardaxoglou, "Analysis of frequency selective surfaces on biased ferrite substrate", *IEEE Antennas and Propagation Society International Symposium. Digest*. [S.l.]: IEEE, 1995, p. 1636–1639.

[25] D. Specht, "A general regression neural network", *IEEE Transactions on Neural Networks*, 1991. Institute of Electrical and Electronics Engineers (IEEE), 1991, v. 2, n. 6, p. 568–576.

[26] X.S. Yang and S. Deb, "Multiobjective cuckoo search for design optimization", *Computers &*

Operations Research, 2013. Elsevier BV, v. 40, n. 6, 2013, pp. 1616–1624.

[27] E.A. Nadaraya, “On estimating regression” Theory of Probability & Its Applications, Society for Industrial & Applied Mathematics (SIAM), v. 9, n. 1, 1964, p. 141–142.

[28] G.S. Watson, “Smooth regression analysis”, Sankhya: The Indian Journal of Statistics, Serie A, v. 26, n. 4, 1964, pp. 359–372.

[29] J. H. Holland, “Adaptation in natural and artificial systems”, University of Michigan Press: Ann Arbor, MI, 1975.

[30] D.E. Goldberg, “Genetic algorithms in search, optimization and machine learning”, Addison-Wesley, 1989.

[31] D. Beasley, D.R. Bull, and R. Martin, “An overview of genetic algorithms: Part 1, fundamentals”, Univ. Comput., 1994, v. 15.

[32] N.A. Kumar, “Efficient hierarchical hybrids parallel genetic algorithm for shortest path routing”, 2014 5th International Conference - Confluence The Next Generation Information Technology Summit (Confluence). [S.l.]: IEEE, 2014.

[33] Z. Konfrist, “Parallel genetic algorithms: advances, computing trends, applications and perspectives”, 18th International Parallel and Distributed Processing Symposium, Proceedings. [S.l.]: IEEE, 2004.

[34] M. Farshbaf, M.R. Feizi-Derakhshi, “Multi-objective optimization of graph partitioning using genetic algorithms”, Third International Conference on Advanced Engineering Computing and Applications in Sciences, Proceedings. [S.l.]: IEEE, 2009.

[35] K. Deb, A. Pratap, S. Agarwal, and T. Meyarivan, “A fast and elitist multiobjective genetic algorithm: NSGA-II”, IEEE Transactions on Evolutionary Computation, v. 6, n. 2, 2002, pp. 182–197.

[36] X.S. Yang and S. Deb, “Cuckoo search: recent advances and applications”, Neural Computing and Applications, Springer Nature, v. 24, n. 1, 2013, pp. 169–174.